PD-118057 contacts the pore helix of hERG1 channels to attenuate inactivation and enhance K^+ conductance

Matthew Perry[a,b], Frank B. Sachse[b,c], Jennifer Abbruzzese[a,b], and Michael C. Sanguinetti[a,b,1]

[a]Department of Physiology, [b]Nora Eccles Harrison Cardiovascular Research and Training Institute, and [c]Department of Bioengineering, University of Utah, Salt Lake City, UT 84112

Edited by David E. Clapham, Harvard Medical School, Boston, MA, and approved September 25, 2009 (received for review June 12, 2009)

Human *ether-a-go-go-related* gene 1 (hERG1) K^+ channels mediate repolarization of cardiac action potentials. Unintended block of hERG1 channels by some drugs can prolong the QT interval and induce arrhythmia. Recently, hERG1 channel agonists were discovered and, based on their mechanisms of action can be classified into two types. RPR260243 [(3*R*,4*R*)-4-[3-(6-methoxy-quinolin-4-yl)-3-oxo-propyl]-1-[3-(2,3,5 trifluorophenyl)-prop-2-ynyl]-piperidine-3-carboxylic acid], a type 1 agonist, binds to residues located near the intracellular end of S5 and S6 transmembrane segments and activates hERG1 channels by a dual mechanism of slowed deactivation and attenuated P-type inactivation. As defined here, type 2 agonists such as PD-118057 [2-(4-[2-(3,4-dichloro-phenyl)-ethyl]-phenylamino)-benzoic acid] attenuate inactivation but do not slow deactivation. At 10 μM, PD-118057 shifted the half-point for inactivation of wild-type hERG1 channels by +19 mV and increased peak outward current by 136%. Scanning mutagenesis and functional characterization of 44 mutant channels expressed in *Xenopus* oocytes was used to identify the major structural determinants of the binding site for PD-118057. Single mutations of residues in the pore helix (F619) or the S6 segment (L646) of hERG1 eliminated agonist activity. Mutation of a nearby residues in the S6 segment (C643, M645) enhanced drug activity, presumably by reducing steric hindrance for drug binding. Molecular modeling indicates that PD-118057 binds to a hydrophobic pocket formed by L646 of one hERG1 subunit and F619 of an adjacent subunit. We conclude that direct interaction of PD-118057 with the pore helix attenuates fast P-type inactivation and increases open probability of hERG1 channels.

activator | potassium channel | voltage clamp

The rapid delayed rectifier K^+ current, I_{Kr} is conducted through channels formed by the tetrameric assembly of human *ether-a-go-go-related* gene 1 (hERG1) α-subunits (1, 2), and plays an important role in normal repolarization of cardiac action potentials. Inherited mutations in hERG1 can cause a loss of channel function leading to long QT syndrome (LQTS) (3) or, very rarely, a gain of channel function leading to short QT syndrome (SQTS) (4). Both disorders are associated with an increased risk of arrhythmia that can cause sudden death.

Drug-induced LQTS is an acquired disorder, caused by unintended block of hERG1 channels by a surfeit of common medications. In the pharmaceutical industry, screening for hERG1 channel block activity has become an important part of the drug development process (5) and has serendipitously led to the discovery of compounds that activate hERG1 and shorten cardiac action potential duration. hERG1 agonists may prove useful as a mechanism-based treatment for LQTS (6, 7); however, safety and efficacy issues have not yet been adequately addressed.

All known hERG1 channel agonists either slow the onset and/or shift the voltage dependence of inactivation to more depolarized potentials (8–10). The effects on other channel gating properties such as the voltage dependence of activation and rate of channel deactivation are variable and drug specific. RPR260243 [(3*R*,4*R*)-4-[3-(6-methoxy-quinolin-4-yl)-3-oxo-propyl]-1-[3-(2,3,5 trifluorophenyl)-prop-2-ynyl]-piperidine-3-carboxylic acid] (6), defined here as a "type 1" hERG1 agonist, binds to a receptor site located at the intracellular ends of the S5 and S6 segments of a single hERG1 subunit to cause a profound slowing of deactivation rate and a positive shift in the voltage dependence of pore (P)-type inactivation gating (9). P-type inactivation of hERG1 is very rapid, and similar to C-type inactivation of other voltage-gated K^+ (Kv) channels, is believed to be caused by a subtle structural change in the selectivity filter (SF) of the outer pore domain (11). Given the location of the binding site for RPR260243, the modification of inactivation gating by this drug must be mediated by a long-range, allosteric effect. PD-118057 [2-(4-[2-(3,4-dichloro-phenyl)-ethyl]-phenylamino)-benzoic acid] enhances hERG1 current without affecting activation or deactivation (7), but its precise mechanism of action is unknown. More recently, Xu et al. (10) reported that the hERG1 agonist PD-307243 (2-[2-(3,4-dichloro-phenyl)-2,3-dihydro-1H-isoindol-5-ylamino]-nicotinic acid) retarded inactivation without altering activation or deactivation gating via modification of the channel pore. We define compounds that enhance current without affecting deactivation as "type 2" hERG1 agonists. Here we characterize the mechanism of channel activation by PD-118057 and use a scanning mutagenesis approach of the hERG1 pore module (S5/pore helix/S6) to identify the molecular determinants of its putative binding site.

Results

Mechanisms of PD-118057 Induced Enhancement of hERG1 Current Magnitude. The effects of PD-118057 on wild-type (WT) hERG1 channels expressed in *Xenopus* oocytes is illustrated in Fig. 1*A*. Channels were activated by a 2-s pulse to +40 mV, then pulsed to a variable test potential (V_t) that ranged from +30 to −140 mV to measure tail currents. Current at +40 mV is small because most channels are in an inactivated state at this potential. At 10 μM, PD-118057 had almost no effect on current elicited by the pulse to +40 mV but markedly enhanced the amplitude of tail currents. The onset of drug effect was slow, requiring ≈30 min to reach steady-state at the lower concentrations examined, and we were unable to fully recover control levels of hERG1 current amplitude after washout. We excluded the possibility of significant current run-up by performing time control experiments with vehicle alone (0.01% DMSO), during which only a small (3.4% ± 3.3%, n = 3) increase in current amplitude was observed. The fully activated *I-V* relationships, defined by the

Author contributions: M.P. and M.C.S. designed research; M.P., J.A., and M.C.S. performed research; M.P., F.B.S., J.A., and M.C.S. analyzed data; and M.P. and M.C.S. wrote the paper.

The authors declare no conflict of interest.

This article is a PNAS Direct Submission.

[1]To whom correspondence should be addressed. E-mail: sanguinetti@cvrti.utah.edu.

This article contains supporting information online at www.pnas.org/cgi/content/full/0906597106/DCSupplemental.

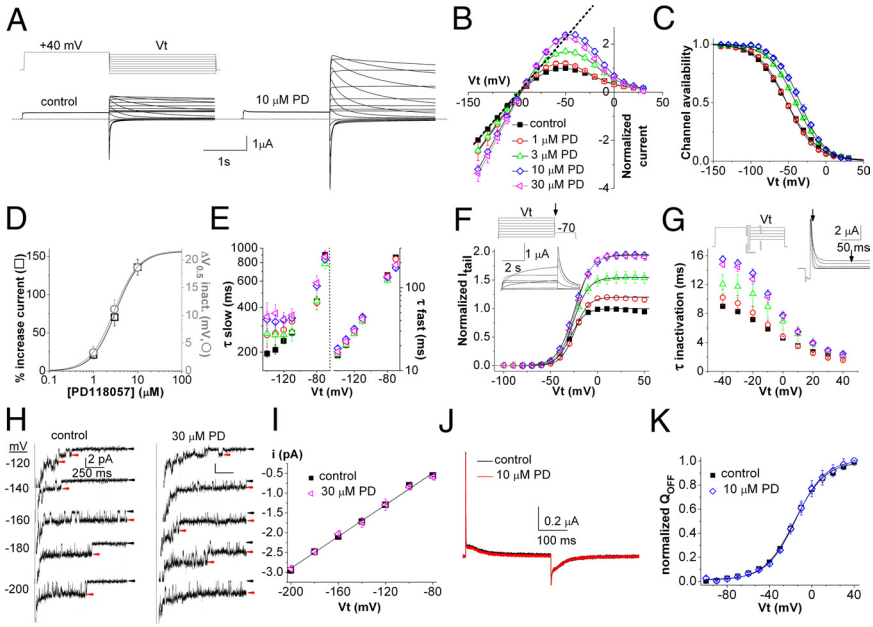

Fig. 1. Effects of PD118057 on the biophysical properties of hERG1 channels. (*A*) hERG1 channel current traces before (control) and after 10 μM PD118057 (PD). Tail currents were elicited with a fully activated *I-V* pulse protocol: a 2-s prepulse to +40 mV was followed by a 2.5-s pulse to a *V*t that was applied in 10-mV increments and varied from −140 to +30 mV (voltage protocol is shown above control current traces). (*B*) Fully activated *I-V* relationships, normalized relative to peak outward value of control tail currents. Dashed line indicates ohmic conductance predicted by linear fit of control currents recorded for *V*t of −110 to −140 mV. (*C*) Voltage dependence of inactivation determined from rectification of the fully activated *I-V* relationship. Data were fit with a Boltzmann function (smooth curves) to determine $V_{0.5}$ and k values (summarized in Table S1). (*D*) [PD-118057]-dependent changes in peak outward currents from *panel B* (open squares; EC_{50} = 3.1 μM, Hill coefficient = 1.9, n = 3–7) and shifts in $V_{0.5}$ for inactivation (open circles; EC_{50} = 2.9 μM, Hill coefficient = 2.0, n = 3–7). (*E*) Time constants for deactivation. Tail currents between −140 and −70 mV were fitted to double exponential function to obtain τslow (*Left*) and τfast (*Right*) for deactivation. (*F*) Effect of PD118057 on the voltage dependence of channel activation. Tail currents were measured at −70 mV following pulses from a *V*t of −80 to +50 mV. Values were normalized to the peak value of the control currents. For control, $V_{0.5}$ for activation was −29.3 ± 1.3 mV and k was 7.3 ± 0.2 mV (n = 7). PD-118057 at 10 μM shifted the relationship by 5.0 ± 1.1 mV ($P < 0.005$). (*G*) PD118057 slows the onset of inactivation. Currents measured between +40 and −40 mV (after 1-s prepulse to +40 mV followed by 10-ms pulse to −110 mV, protocol show at *top left*) were fitted to a single exponential function (area fitted shown in example current in *top right*). Symbols in *B, C, E, ,F* and *G* are as follows: control (filled squares), 1 μM (open circles), 3 μM (open triangles), 10 μM (open diamonds), and 30 μM (open triangles) PD-118057. (*H*) Single-channel activity recorded in cell-attached patches from an untreated oocyte and an oocyte incubated for 30 min with 30 μM drug. Currents were elicited at the indicated *V*t immediately after a 200-ms prepulse to +40 mV. Patches contained multiple channels that deactivated until only one or two were visible. Black arrows indicate closed state and red arrows indicate open states of individual channels. (*I*) *I-V* relationship for hERG1. Single-channel conductance (γ) determined by linear regression analysis was 19.8 ± 0.6 pS for control oocytes (n = 3–4 patches per data point), and 20.1 ± 0.9 pS for oocytes treated with 30 μM drug for 20–40 min (n = 4–8 patches per data point). (*J*) PD-118057 does not alter kinetics or magnitude of hERG1 gating currents. Traces of gating currents recorded before and after treatment of a single oocyte with 10 μM drug for 20 min are superimposed. Holding potential was −110 mV and *V*t was +40 mV. (*K*) Q_{OFF}-V relationships normalized to the value at +40 mV under control conditions for each oocyte. Off gating charge (Q_{OFF}) was determined by integration of the off gating currents measured at −110 mV. Before drug, the average Q_{OFF} after a pulse to +40 mV was −4.7 +1.1 μC (n = 4). Data were fit with a Boltzmann function (smooth curves). For control, $V_{0.5}$ = −15.7 ± 1.9 mV, k = 14.4 ± 1.1 mV; for PD-118057, $V_{0.5}$ = −14.5 ± 1.8 mV, k = 14.2 ± 1.3 mV (n = 4).

plot of peak tail current amplitude as a function of *V*t for control and several concentrations of PD-118057, are shown in Fig. 1*B*. The drug-induced enhancement of hERG1 current magnitude was concentration dependent between 1 and 10 μM, and the peak outward currents were enhanced by 136.0% ± 9.5% (n = 7) with 10 μM. The effects of 30 μM drug were similar to 10 μM except for *V*t greater than −50 mV, for which currents were slightly decreased. Inward rectification of the fully activated *I-V* relationship is caused by rapid P-type inactivation of hERG1 channels. Deviation of this relationship from linearity (indicated in Fig. 1*B* for control conditions by dotted line) provides an estimate for the voltage dependence of inactivation (Fig. 1*C*). In control conditions, the $V_{0.5}$ for inactivation was −52.8 ± 1.7 mV (n = 7). PD shifted the $V_{0.5}$ by +3.3 ± 1.1 mV at 1 μM (n = 3), +11.1 ± 1.7 mV at 3 μM (n = 4), and +18.6 ± 1.3 mV at 10 μM (n = 7). The EC_{50} for the shift in the $V_{0.5}$ for inactivation was 2.9 μM, similar to the EC_{50} of 3.1 μM obtained by measuring changes in peak outward current of the fully activated *I-V* relationship (Fig. 1*D*). The Hill coefficient was ≈2 for both measures of drug activity, indicating a positively cooperative binding reaction and suggesting the possibility of two binding sites/channel. PD-118057 had relatively minor effects on the rate of hERG1 deactivation (Fig. 1*E*). However, the drug caused a small depolarizing shift in the voltage dependence of activation (Fig. 1*F*) and as shown in Fig. 1*G*, a concentration-dependent slowing of the onset of inactivation (e.g., at 10 μM, time constant was increased from 4.6 ± 0.2 ms to 7.8 ± 0.4 ms at 0 mV; n = 7, $P < 0.0001$).

Single hERG1 channel activity was measured in cell-attached patches of oocytes that were bathed in control media or in media containing 30 μM PD-118057 for 20–40 min (Fig. 1*H*). The conductance (γ) of single hERG1 channels was identical under both conditions (Fig. 1*I*). PD-118057 (10 μM for 20 min) also had no effect on the kinetics or magnitude of hERG1 gating currents measured using the COVG voltage clamp technique (Fig. 1*J*) or the magnitude of OFF gating charge (Q_{OFF}) at any *V*t examined (Fig. 1*K*).

To further explore the role of altered inactivation as a mechanism for agonist activity, the effect of PD-118057 on the noninactivating G628C/S631C hERG1 mutant channel was determined. The mutated residues in this channel are located near or within the SF, and the resulting disulfide bond between the

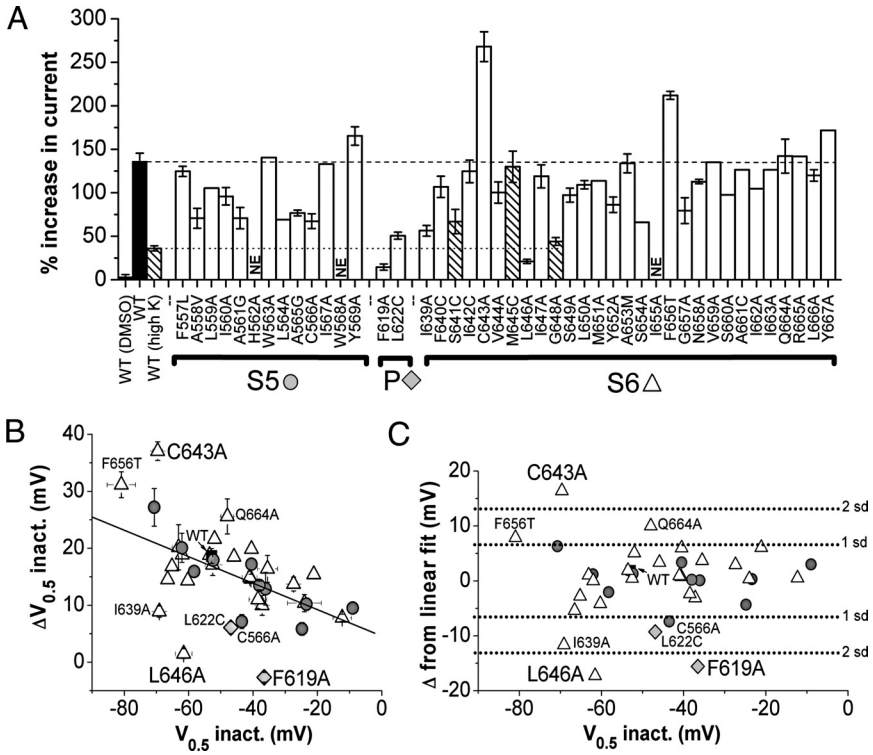

Fig. 2. Scanning mutagenesis of hERG1 pore module defines molecular determinants of hERG1 channel sensitivity to PD-118057. (*A*) Bar graph summarizing percent increase in current magnitude induced by 10 μM PD-118057 on hERG1 channels with indicated point mutations in the S5, pore (P), or S6 domains. Currents were measured at the peak of the fully activated *I-V* relationship for WT and mutant channels. Vehicle control (DMSO) had no effect. NE, nonexpressing channels. High K (hatched bars) indicates that currents were measured in oocytes bathed in a 20-mM $[K^+]_e$ solution (see *Methods*). (*B*) Plot of shift in inactivation $V_{0.5}$ ($\Delta V_{0.5}$) induced by 10-μM PD118057 induced as a function of the $V_{0.5}$ measured in absence of drug. Symbols indicate WT hERG1 (filled squares), or location of point mutation in the S5 (filled circles), pore (filled triangles), or S6 (open triangles). Line represents best fit of data to a linear function. (*C*) Deviation of $\Delta V_{0.5}$ from that predicted by the linear fit shown in *panel B* was calculated for each mutant channel and plotted against initial $V_{0.5}$ inactivation under control conditions. Mutations that induced a change of greater than ± 1 or $\pm$ 2 standard deviations (SD) from the mean are indicated. Symbols are the same as in *B*.

introduced Cys residues (12) eliminates inactivation and reduces K^+ selectivity of hERG1 channels (13). At 10 μM, PD-118057 increased WT hERG1 current but had no significant effect on currents conducted by G628C/S631C mutant channels [supporting information (SI) Fig. S1]. Two other mutations of hERG1 that diminish inactivation without affecting ion selectivity (e.g., N588K or S620T) reduced the effects of 10 μM PD-118057 by approximately half compared with WT channels (Fig. S1). Elevated $[K^+]_e$ diminishes P-type inactivation of hERG1 (14). Therefore, the effects of 10 μM drug on WT channels were compared when $[K^+]_e$ was elevated from 2 mM to 20 mM. Elevated $[K^+]_e$ reduced the agonist activity of the drug by 36% (Fig. S2). The lack of agonist effect on noninactivating hERG1 mutant channels and the attenuated effects with high $[K^+]_e$ confirm that reduced P-type inactivation is an important, but not the only, mechanism for the agonist activity of PD-118057. At -120 mV and more negative potentials, where recovery from inactivation is complete, tail currents were also enhanced by the drug, albeit by less than half the increase induced for peak outward currents (Fig. 1*A* and *B*). The increase in peak inward tail currents reached a maximum of 61.2% $\pm$ 3.3% (n = 7) at -140 mV with 10 μM PD-118057. Moreover, the shift in inactivation can account for only half, approximately, of the observed increase in outward current magnitude at the peak of the fully activated *I-V* relationships summarized in Fig. 1*B*. Other possible mechanisms of agonist activity include an increase in the number of channels (N) recruited to the cell surface, or an increase in single-channel conductance (γ) or open probability (P_o). However, the drug did not alter γ (Fig. 1*I*) and had no effect on the peak value of Q_{OFF} (Fig. 1*K*), indicating no effect on N. Peak inward tail current is defined as $I_{hERG1} = \gamma(V\text{t-}V\text{rev})\cdot N\cdot P_o$, where *V*rev is the reversal potential for current. By process of elimination we conclude that PD118057 must increase P_o. However, because of significant run-down of single-channel activity in patches and variability in P_o over time, this effect was not verified directly.

Molecular Determinants of PD-118057 Binding. To identify the putative binding site for PD-118057, we performed scanning mutagenesis of the hERG1 pore module (Fig. 2*A*). We initially focused on S5 and S6, the region of interaction with RPR260243 (9). Most residues were substituted with Ala or Cys (or Ala to Gly/Val); however, in a few cases, alternative substitutions were made to enhance channel expression (see *Methods*). The fully activated *I-V* relationship was determined for mutant channels in the absence and presence of 10 μM PD-118057; and drug response, quantified as percent increase in the peak outward tail current, is summarized in Fig. 2*A*. The inactivation parameters ($V_{0.5}$, k) of the mutant channels in the absence and presence of 10 μM drug are summarized in Table S1. Of the 42 scanned residues in the S5/S6 segments, three mutant channels were nonfunctional or expressed at too low a level for characterization (denoted as "NE" in Fig. 2*A*). Three other mutations (S641C, M645C, and G648A) induced strong inactivation; therefore, currents for these mutant channels were recorded using a high $[K^+]_e$ solution to reduce inactivation and to enhance current magnitude. The responses of S641C and G648A channels to 10 μM drug was similar to those of WT channels, whereas the increase of M645C current was three times greater (Fig. 2*A*, Table S1). The drug sensitivities of the remaining 36 mutant channels varied somewhat, but some of this variation can be

PHARMACOLOGY

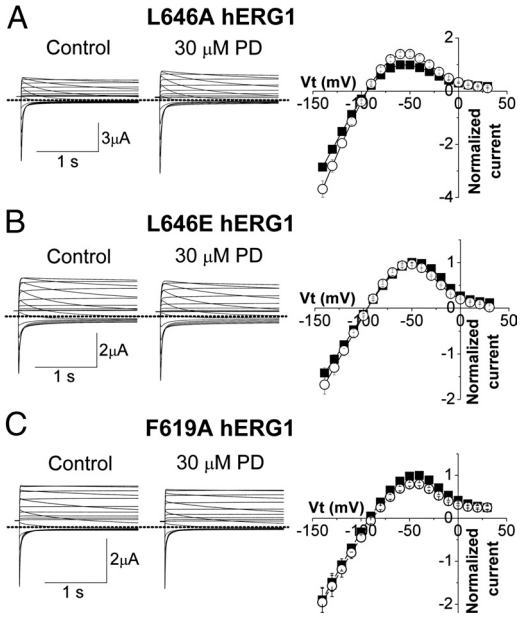

Fig. 3. Mutation of Leu-646 or Phe-619 reduces or eliminates hERG1 sensitivity to PD-118057. (*A*) (*Left*) L646A channel tail currents (elicited as described in Fig. 1*A*) before (control) and after 30 μM PD-118057. (*Right*) Fully activated *I-V* relationships measured in control (filled squares) and after 30 μM PD-118057 (open circles). Currents were normalized relative to peak outward value of control tail currents. (*B* and *C*) Current traces (*Left*) and fully activated *I-V* relationships (*Right*) for L646E (*B*) and F619A (*C*) hERG1 channels.

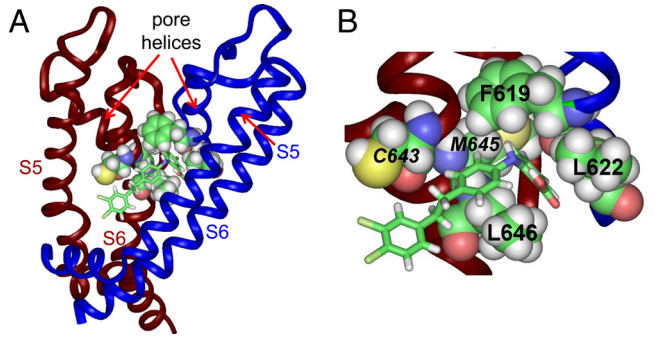

Fig. 4. PD-118057 docked to a homology model of the pore module of hERG1. (*A*) Side view of the pore region of two adjacent hERG1 subunits. (*B*) Amplified view of the drug binding region. Drug is portrayed in stick mode. Residues identified by scanning mutagenesis as the most important for interaction with PD-118057 are shown in space-fill mode. C643, M645, and L646 are located in S6 of subunit colored red; F619 and L622 are located in the pore helix of subunit colored blue. Mutations of C643 and M645 enhanced, whereas mutations of F619, L622, and L646 diminished, drug sensitivity. S5 helix of the blue subunit has been removed for clarity. The PDB file for PD-118057 docked to the two-subunit model of hERG1 is available (Dataset S1).

accounted for by the effect of the mutation itself on inactivation gating.

The drug-induced shift in the $V_{0.5}$ for inactivation varied as an inverse function of the initial $V_{0.5}$ measured under control conditions (Fig. 2*B*). To compensate for this effect, the deviation of the drug-induced shift in $V_{0.5}$ for inactivation from the linear relationship plotted in Fig. 2*B* was calculated and plotted against initial $V_{0.5}$ in Fig. 2*C*. The deviation from linearity was greater than +1 SD from the mean for F656T and Q664A, and greater than +2 SD for C643A, indicating enhanced drug sensitivity. Although the shift in $V_{0.5}$ for Q664A channels was significantly greater than for WT, the percent increase in current was not altered (Fig. 2*A*). Thus, Q664 is not likely to interact with the drug. In contrast, C643A current magnitude was increased by 268% ± 17% with 10 μM drug, and this effect was accompanied by a shift in $V_{0.5}$ for inactivation of +37.0 ± 1.6 mV (n = 5, Fig. S3). As discussed below, F656 is likely a binding residue for another site that mediates the blocking activity of PD-118057 at higher concentrations. The deviation from linearity for the relationship plotted in Fig. 2*B* was greater than −1 SD for C566A and I639A and greater than −2 SD for L646A, indicating reduced drug sensitivity. At the maximal soluble concentration of 30 μM, the drug increased peak outward current of L646A channels by 41.9% ± 8.0% and shifted $V_{0.5}$ for inactivation by +4.7 ± 1.7 mV (n = 3, Fig. 3*A*). We hypothesized that, if L646 constituted an important hydrophobic binding residue, substitution with a charged amino acid would reduce sensitivity more than the Ala substitution. Indeed, current from L646E mutant channels were not enhanced by 30 μM drug and in fact were reduced by 6.2% ± 3.6% (n = 3, Fig. 3*B*), indicating a >30-fold reduction in sensitivity compared with WT hERG1. Thus, scanning mutagenesis of the S5/S6 segments of hERG1 identified three mutations (C643A, M645C, and L646A) that strongly modified drug sensitivity.

A homology model of the hERG1 channel based on the open state of the Kv1.2 channel structure (15) predicts that C643, M645, and L646 in S6 are in close proximity to residues F619 and L622 in the pore helix of an adjacent subunit. Therefore, we examined the effect of mutating these two pore helix residues. The mutation F619A eliminated the agonist activity of 10 μM PD-118057 (Fig. 2*A*) and at 30 μM, current was reduced by 20.2% ± 3.9%, (n = 4; Fig. 3*C*), indicating that PD-118057 is a partial agonist. L622A channels were nonfunctional, but L622C hERG1 channel currents were robust and exhibited reduced sensitivity to the drug. At 10 μM, PD-118057 enhanced L622C current magnitude by 50.7 ± 4.0% (Fig. 2*A*) with a shift in $V_{0.5}$ inactivation of +6.1 ± 1.0 mV (n = 5, Fig. S3). In summary, four mutations (F619A, L622C, I639A, and L646A) decreased sensitivity, and two mutations (C643A and M645C) enhanced sensitivity, of hERG1 channels to PD-118057.

Molecular Model of PD-118057 Docking to hERG1. Molecular modeling was used to dock PD-118057 to the Kv1.2-based homology model of the hERG1 channel pore. Fig. 4 shows the preferred drug docking to the pore region of two adjacent subunits. Docking was initiated from 200 random configurations of the drug and allowed for binding positioned at a maximal distance of 15 Å from C643 of the S6 of hERG1 subunit colored red in Fig. 4. The putative binding site for PD-118057 lies within a cavity created by the S6 helix of one subunit (colored red in Fig. 4*A*) and the pore helix of an adjacent subunit (colored blue in Fig. 4*A*). The benzoic acid of PD interacts with F619 and L622 residues located at the base of the pore helix on one subunit, and a hydrophobic interaction occurs between the central phenyl group of the drug and L646 on the S6 helix of the adjacent subunit. Mutating L646 to a negatively charged residue (L646E) is predicted to attenuate drug binding by occluding the cavity (shown in Fig. S4). C643 and M645 are also in close proximity to the bound drug and mutations of either residue enhanced drug sensitivity. Thus, these residues might sterically hinder drug binding. Another residue identified as potentially important by scanning mutagenesis, I639, is located too far away to interact with the drug in this docking. Moreover, because of the limitations of the scanning mutagenesis, we cannot exclude the possibility that other residues might contribute to the stabilization of PD-118057 binding. For example, relatively conservative mutations (e.g., Val to Ala) may not appreciably alter the affinity of drug binding.

Discussion

Two classes of hERG1 channel activators can be described based upon their mechanisms of action. Type 1 agonists such as

RPR260243 enhance current magnitude by attenuating P-type inactivation and slowing deactivation. Type 2 agonists such as PD-118057 attenuate inactivation and enhance conductance by another mechanism, tentatively identified here as an increase in P_o of single channels. The mapping of the putative binding sites for RPR260243 (9) and PD-118057 provide structural insights into the basis of these different mechanisms of action. Residues that constitute the putative RPR260243 binding site are located at the intracellular ends of the S5 helix (L553, F557) and an adjacent region of the S6 helix (N658, V659) of a single hERG1 subunit (9). Drug binding at this location could hinder the bending of S6 helices required for channel closure and thus, slow deactivation. Our findings suggest that PD-118057 binds to a distant hydrophobic pocket formed by residues located on the pore helix and a nearby region of S6 and therefore, does not directly affect deactivation. The location of the binding site for these two drugs does not readily explain their similar effects on inactivation gating. P-type inactivation of Kv channels, including hERG1, is induced by a change in the conformation of the SF that prevents K^+ conductance. The voltage dependence of P-type inactivation is linked to the S4 voltage sensor (16); however, point mutations in the S5 (17) and S6 (Table S1) helices alter the voltage dependence of P-type inactivation, suggesting that these regions couple S4 movement to a conformational change in the SF. PD-118057 interacts with L646 in the S6 domain of one subunit and by F619 and L622 in the pore helix of an adjacent subunit. The drug could directly hinder the coupling between S4 and the SF or could itself produce a conformational change in the pore helix that is less favorable to the onset of P-type inactivation. For the G628C/S631C mutant channel, the disulfide bond formed between C628 and C631 alters the configuration of the SF (12) and completely removes inactivation; this could either disrupt the drug binding site or prevent the changes in SF function induced by drug in the WT channel. In contrast to these direct actions of PD-118057 on the SF, RPR260243 must modify inactivation gating by an indirect, allosteric mechanism mediated by restricted S5/S6 coupling of S4 movement to a conformational change of the SF.

The location of the proposed hydrophobic binding site in hERG1 for PD-118057 resembles the site proposed for retigabine binding to KCNQ channels. Two key residues for retigabine binding to KCNQ3 channels (L314 and L338) (18) align with two Leu residues (L622 and L646) in hERG1. The agonist activity of retigabine is mainly attributed to a shift in the voltage dependence of activation to more hyperpolarized potentials, but an accelerated activation and slowed deactivation (19, 20), and increased P_o of single channels (21) also contributes to its agonist action.

In addition to the prominent agonist activity of PD-118057, a blocking effect was revealed at a concentration of 30 μM. Block was voltage dependent, occurring only at potentials positive to −50 mV, and was most apparent for L646E and F619A mutant channels that were completely insensitive to the agonist effect, suggesting that distinct binding sites mediate the agonist and antagonist effects. F656 in S6 is the most important residue for binding of hERG1 channel blockers (22, 23). This residue may also interact with PD-118057 to mediate blockade, consistent with our finding that F656T channels exhibited enhanced sensitivity to the drug (Fig. S3).

In summary, PD-118057 interacts with residues located in the pore helix of one hERG1 subunit and the N-terminal half of the S6 helix in an adjacent subunit to attenuate inactivation and increase P_o. In contrast, RPR260243 binds to the intracellular ends of S5 and S6 of a single subunit and slows deactivation in addition to reducing inactivation. Characterizing the variable mechanisms of action and binding sites for hERG1 agonists will facilitate the future development of alternative therapies for LQTS.

Materials and Methods

Channel Mutagenesis and Expression in *Xenopus* Oocytes. *HERG1* (*KCNH2*, isoform 1a, NCBI Reference Sequence: NM_000238.2) (24), was cloned into the pSP64 oocyte expression vector, and mutations were introduced using the QuikChange mutagenesis kit (Stratagene, La Jolla, CA). Residues F557-Y569 in S5 and I639-Y667 in S6 were mutated to Ala or Cys (to Gly or Val for Ala residues). Three mutations (H562A, W568A, and I655A) expressed poorly and were not further studied. For some residues, alternate substitutions were introduced to enhance expression (indicated in Fig. 2*A*). For example, for H562, four additional substitutions (C, K, and T, N) produced nonfunctional channels. cRNA was prepared by in vitro transcription with mMessage mMachine SP6 kit (Ambion, Austin, TX) after linearization of the vector plasmid with EcoR1. The isolation, culture, and injection of oocytes with cRNA were performed as described (25, 26).

Voltage Clamp. Currents were recorded from oocytes 1–5 days after cRNA injection by using the two-electrode voltage-clamp technique and a Geneclamp 500 amplifier (Molecular Devices, Sunnyvale, CA) as described (25). Gating currents were measured using the cut-open oocyte Vaseline gap (COVG) method as described (27). Single hERG1 channel currents were measured in cell-attached patches as described (28). For all experiments, digitized data were analyzed off-line with pCLAMP9 (Molecular Devices, Sunnyvale, CA) and ORIGIN 8 (OriginLab, Northhampton, MA) software. Data are expressed as mean ± standard error (n = number of oocytes). (For a detailed description of voltage clamp techniques, see *SI Methods*.)

Molecular Modeling. Modeling and docking were performed with the Insight II modules Homology, Builder and Docking (version 8.2, Accelrys, San Diego, CA). (For a detailed description of the modeling, see *SI Methods*.)

Solutions and Drugs. For two-microelectrode voltage-clamp experiments, the extracellular solution contained the following (in mM): 96 NaCl, 2 KCl, 1 $CaCl_2$, 5 Hepes, and 2 $MgCl_2$ (pH 7.6). For gating current experiments, the extracellular solution in the top and guard compartments contained the following (in mM): 120 TEA-Mes (tetraethylammonium 4-morpholineethanesulfonic acid), 2 Ca-Mes, 10 Hepes, and 10 μM terfenadine (pH 7.4), and the intracellular solution in the bottom compartment contained (in mM) 120 TEA-Mes, 2 EDTA, and 10 Hepes (pH 7.4). For single-channel experiments, patch pipettes contained the following (in mM): 140 K-gluconate, 10 Hepes, 2 $MgCl_2$, and 0.1 $CaCl_2$ (pH 7.2), and the extracellular solution contained (in mM) 140 KCl, 10 Hepes, 2 $MgCl_2$, and 0.1 $CaCl_2$ (pH 7.2)

PD-118057 was kindly donated by Pfizer (Groton, CT) and also purchased from Sigma-Aldrich (St. Louis, MO). Drug solutions were prepared daily by dilution of a 10 mM DMSO stock solution of PD-118057. Each oocyte was treated with a single concentration of drug.

ACKNOWLEDGMENTS. We thank Vivek Garg for assistance with single-channel recording and Kam Hoe Ng for technical assistance. This work was supported by National Institutes of Health/National Heart, Lung, and Blood Institute grant HL055236.

1. Sanguinetti MC, Jiang C, Curran ME, Keating MT (1995) A mechanistic link between an inherited and an acquired cardiac arrhythmia: *HERG* encodes the I_{Kr} potassium channel. *Cell* 81:299–307.
2. Trudeau M, Warmke JW, Ganetzky B, Robertson GA (1995) HERG, A human inward rectifier in the voltage-gated potassium channel family. *Science* 269:92–95.
3. Curran ME, et al. (1995) A molecular basis for cardiac arrhythmia: *HERG* mutations cause long QT syndrome. *Cell* 80:795–803.
4. Brugada R, et al. (2004) Sudden death associated with short-QT syndrome linked to mutations in HERG. *Circulation* 109:30–35.
5. Sanguinetti MC, Mitcheson JS (2005) Predicting drug-hERG channel interactions that cause acquired long QT syndrome. *Trends Pharmacol Sci* 26:119–124.
6. Kang J, et al. (2005) Discovery of a small molecule activator of the human ether-a-go-go-related gene (HERG) cardiac K^+ channel. *Mol Pharmacol* 67:827–836.
7. Zhou J, et al. (2005) Novel potent human ether-a-go-go-related gene (hERG) potassium channel enhancers and their in vitro antiarrhythmic activity. *Mol Pharmacol* 68:876–884.
8. Casis O, Olesen SP, Sanguinetti MC (2006) Mechanism of action of a novel human ether-a-go-go-related gene channel activator. *Mol Pharmacol* 69:658–665.
9. Perry M, Sachse FB, Sanguinetti MC (2007) Structural basis of action for a human ether-a-go-go-related gene 1 potassium channel activator. *Proc Natl Acad Sci USA* 104:13827–13832.
10. Xu X, Recanatini M, Roberti M, Tseng GN (2008) Probing the binding sites and mechanisms of action of two human ether-a-go-go-related gene channel activators, 1,3-bis-(2-hydroxy-5-trifluoromethyl-phenyl)-urea (NS1643) and 2-[2-(3,4-dichlorophenyl)-2,3-dihydro-1H-isoindol-5-ylamino]-nicotinic acid (PD307243). *Mol Pharmacol* 73:1709–1721.

11. Kiss L, Korn SJ (1998) Modulation of C-type inactivation by K^+ at the potassium channel selectivity filter. *Biophys J* 74:1840–1849.
12. Stansfeld PJ, et al. (2008) Insight into the mechanism of inactivation and pH sensitivity in potassium channels from molecular dynamics simulations. *Biochemistry* 47:7414–7422.
13. Smith PL, Baukrowitz T, Yellen G (1996) The inward rectification mechanism of the HERG cardiac potassium channel. *Nature* 379:833–836.
14. Wang S, Morales MJ, Liu S, Strauss HC, Rasmusson RL (1996) Time, voltage and ionic concentration dependence of rectification of h-*erg* expressed in *Xenopus* oocytes. *FEBS Lett* 389:167–173.
15. Long SB, Campbell EB, Mackinnon R (2005) Crystal structure of a mammalian voltage-dependent Shaker family K^+ channel. *Science* 309:897–903.
16. Piper DR, Hinz WA, Tallurri CK, Sanguinetti MC, Tristani-Firouzi M (2005) Regional specificity of human ether-a-go-go-related gene channel activation and inactivation gating. *J Biol Chem* 280:7206–7217.
17. Ju P, et al. (2009) The pore domain outer helix contributes to both activation and inactivation of the HERG K^+ channel. *J Biol Chem* 284:1000–1008.
18. Lange W, et al. (2009) Refinement of the binding site and mode of action of the anticonvulsant Retigabine on KCNQ K^+ channels. *Mol Pharmacol* 75:272–280.
19. Schenzer A, et al. (2005) Molecular determinants of KCNQ (Kv7) K^+ channel sensitivity to the anticonvulsant retigabine. *J Neurosci* 25:5051–5060.
20. Wuttke TV, Seebohm G, Bail S, Maljevic S, Lerche H (2005) The new anticonvulsant retigabine favors voltage-dependent opening of the Kv7.2 (KCNQ2) channel by binding to its activation gate. *Mol Pharmacol* 67:1009–1017.
21. Tatulian L, Brown DA (2003) Effect of the KCNQ potassium channel opener retigabine on single KCNQ2/3 channels expressed in CHO cells. *J Physiol* 549:57–63.
22. Fernandez D, Ghanta A, Kauffman GW, Sanguinetti MC (2004) Physicochemical features of the hERG channel drug binding site. *J Biol Chem* 279:10120–10127.
23. Mitcheson JS, Chen J, Lin M, Culberson C, Sanguinetti MC (2000) A structural basis for drug-induced long QT syndrome. *Proc Natl Acad Sci USA* 97:12329–12333.
24. Warmke JW, Ganetzky B (1994) A family of potassium channel genes related to *eag* in *Drosophila* and mammals. *Proc Natl Acad Sci USA* 91:3438–3442.
25. Stühmer W (1992) Electrophysiological recording from *Xenopus* oocytes. *Methods Enzymol* 207:319–339.
26. Goldin AL (1991) Expression of ion channels by injection of mRNA into Xenopus oocytes. *Methods Cell Biol* 36:487–509.
27. Piper DR, Varghese A, Sanguinetti MC, Tristani-Firouzi M (2003) Gating currents associated with intramembrane charge displacement in HERG potassium channels. *Proc Natl Acad Sci USA* 100:10534–10539.
28. Zou A, Curran ME, Keating MT, Sanguinetti MC (1997) Single HERG delayed rectifier K^+ channels in *Xenopus* oocytes. *Am J Physiol* 272:H1309–H1314.